Geoscience Frontiers 10 (2019) 1701–1713

HOSTED BY

ELSEVIER

Contents lists available at ScienceDirect

China University of Geosciences (Beijing)

Geoscience Frontiers

journal homepage: www.elsevier.com/locate/gsf

Research Paper

Contrasting sorption behaviours affecting groundwater arsenic concentration in Kandal Province, Cambodia

Laura A. Richards [a], Maria J. Casanueva-Marenco [a,b], Daniel Magnone [c], Chansopheaktra Sovann [d], Bart E. van Dongen [a], David A. Polya [a,*]

[a] School of Earth and Environmental Sciences and Williamson Research Centre for Molecular Environmental Science, The University of Manchester, Williamson Building, Oxford Road, Manchester, M13 9PL, UK
[b] Department of Analytical Chemistry, Institute of Biomolecules, Faculty of Sciences, University of Cádiz, Cádiz, Spain
[c] School of Geography, University of Lincoln, Brayford Pool, Lincoln, Lincolnshire, LN6 7TS, UK
[d] Department of Environmental Science, Royal University of Phnom Penh, Phnom Penh, Cambodia

ARTICLE INFO

Article history:
Received 22 November 2017
Received in revised form
28 December 2018
Accepted 25 February 2019
Available online 10 April 2019

Keywords:
Arsenic
Groundwater
Partial equilibrium
Sorption
Water-rock interactions
Cambodia

ABSTRACT

Natural arsenic (As) contamination of groundwater which provides drinking water and/or irrigation supplies remains a major public health issue, particularly in South and Southeast Asia. A number of studies have evaluated various aspects of the biogeochemical controls on As mobilization in aquifers typical to this region, however many are predicated on the assumption that key biogeochemical processes may be deduced by sampled water chemistry. The validity of this assumption has not been clearly established even though the role of sorption/desorption of As and other heavy metals onto Fe/Mn (hydr) oxides is an important control in As mobilization. Here, selective chemical extractions of sand-rich and clay-rich sediments from an As-affected aquifer in Kandal Province, Cambodia, were undertaken to explore the potential role of partial re-equilibrium through sorption/desorption reactions of As and related solutes (Fe, Mn and P) between groundwater and the associated solid aquifer matrix. In general, groundwater As is strongly affected by both pH and *Eh* throughout the study area. However, contrasting sorption behaviour is observed in two distinct sand-dominated (T-Sand) and clay dominated (T-Clay) transects, and plausibly attributed to differing dominant lithologies, biogeochemical and/or hydrogeological conditions. Sorption/desorption processes appear to be re-setting groundwater As concentrations in both transects, but to varying extents and in different ways. In T-Sand, which is typically highly reducing, correlations suggest that dissolved As may be sequestered by sorption/re-adsorption to Fe-bearing mineral phases and/or sedimentary organic matter; in T-Clay *Eh* is a major control on As mobilization although binding/occlusion of Fe-bearing minerals to sedimentary organic matter may also occur. Multiple linear regression analysis was conducted with groups categorised by transect and by *Eh*, and the output correlations support the contrasting sorption behaviours encountered in this study area. Irrespective of transect, however, the key biogeochemical processes which initially control As mobilization in such aquifers, may be "masked" by the re-setting of As concentrations through in-aquifer sorption/desorption processes.

© 2019, China University of Geosciences (Beijing) and Peking University. Production and hosting by Elsevier B.V. This is an open access article under the CC BY-NC-ND license (http://creativecommons.org/licenses/by-nc-nd/4.0/).

1. Introduction

Arsenic (As) contamination of groundwater in sedimentary aquifers of South and South East Asia has been recognized as causing "the greatest mass poisoning of a population in human history" (Smith et al., 2000). High As concentrations in groundwater have exceeded the World Health Organization (WHO) provisional guide value for drinking water (10 μg/L) by one or even two orders of magnitude (e.g. Ravenscroft et al., 2009; Polya et al., 2010; World Health Organization, 2011; Phan et al., 2014; Polya and Lawson, 2015; Polya and Middleton, 2017) including in some areas of West Bengal, Bangladesh, Cambodia and other countries of the region, where groundwater is a major source of drinking and cooking water

* Corresponding author.
E-mail address: david.polya@manchester.ac.uk (D.A. Polya).
Peer-review under responsibility of China University of Geosciences (Beijing).

https://doi.org/10.1016/j.gsf.2019.02.010
1674-9871/© 2019, China University of Geosciences (Beijing) and Peking University. Production and hosting by Elsevier B.V. This is an open access article under the CC BY-NC-ND license (http://creativecommons.org/licenses/by-nc-nd/4.0/).

for many rural and peri-urban dwellers. Studies of As-contaminated aquifers around the world have demonstrated that As concentrations can be controlled by complex environmental conditions and biogeochemical processes, including microbially-mediated redox reactions, adsorption/desorption, precipitation or co-precipitation and dissolution (e.g. Smedley and Kinniburgh, 2002; Islam et al., 2004; Ravenscroft et al., 2009; Al Lawati et al., 2012a,b, 2013; Wang et al., 2014; Kim et al., 2015; Polya and Lawson, 2015). The relative extent to which these various biogeochemical processes control the concentration of As in groundwater is important when considering models of As release and transport including in the context of predictive models of future changes in arsenic hazard (Michael and Voss, 2008; Radloff et al., 2011; van Geen et al., 2013). Understanding the extent to which sorption behaviours of sediments may control groundwater As distribution is important for interpreting groundwater geochemical data, guiding further research efforts as well as ultimately informing policy.

Adsorption/desorption is an important process controlling the mobility of inorganic contaminants in aquifers, sediments and soils (Goldberg et al., 2007). In particular, adsorption of As onto (hydr) oxides or carbonates, and desorption of As into aqueous solution as regulated by pH, redox potential and the presence of competitive ions, have been proposed as mechanisms regulating the natural mobilization and distribution of groundwater As (e.g. Peters, 2008; Javed et al., 2013; Mai et al., 2014; Diwakar et al., 2015; Yang et al., 2015). Arsenic adsorbed and sequestered on Fe/Mn (hydr)oxides is one of the most common reservoirs of this element in some sedimentary basins of South and Southeast Asia (Xie et al., 2009). The reducing nature of some groundwaters can facilitate the reduction of As(V) to As(III), leading to possible desorption of As, especially as As(III) may be less strongly adsorbed by ferric (hydr)oxides than As(V) (Mayorga et al., 2013; Paul et al., 2015), although it should be noted that this may not always be the case (Dixit and Hering, 2003). Changes in the sorption capacity of ferric (Fe(III)) (hydr)oxides and their reductive dissolution are two of the major processes controlling As concentrations (Smedley and Kinniburgh, 2002; Kim et al., 2012; Yadav et al., 2015).

Enhanced preservation of organic matter (OM) occurs in marine and terrestrial sedimentary environments through the adsorption of Fe hydroxide minerals and associated trace metals (notably Mn). In some marine sediments, up to 22% ± 9% of the OM is directly bound to the reactive Fe phases (Lalonde et al., 2012) and in some soils sorbed OM is postulated to "mask" mineral surfaces, leading to the composition of OM being a primary control of sorption behaviours (Kaiser and Guggenberger, 2000). The surface OM exhibits a different composition to bulk OM and it is hypothesised that minerals interact with the OM through co-precipitation or chelation (Johnson et al., 2015). This absorption may be strongly linked to the grain-size of sediments as these are surface bonds (Roy et al., 2013). Lignin and humin (proto kerogen) compounds have been shown to bond to Fe minerals in this process (Kaiser and Guggenberger, 2000; Vandenbroucke and Largeau, 2007). Given the importance of absorption in As contaminated aquifers it is possible that OM absorption is an important feature in the sequestration of aqueous As.

Many studies of the origin of high As in shallow reducing groundwater are predicated by an explicit or implicit assumption that the nature of key biogeochemical processes may be deduced from sampled water chemistry. However, since groundwater systems are dynamic and As concentrations, in particular, may partially re-equilibrate through sorption/desorption processes with the sediments through which they flow, it remains unclear the degree to which such approaches are valid. This is particularly a concern where groundwater residence times of on order of years to hundreds of years or more in contrast to sorption/desorption equilibration timescales which are typically more on the order of hours to hundreds of hours. Thus, the aim of this study was to assess the importance of such partial re-equilibration in re-setting groundwater As concentrations, in well-studied As-prone shallow reducing aquifers in Cambodia. The quantitative importance of these processes might reasonably be expected to depend in part on groundwater pH and *Eh* and sediment grain size (as a proxy for specific surface area) as well as on the concentrations of weakly and more strongly bound As and related components, notably Fe, Mn, and P in the solid aquifer materials. Accordingly, the objectives were to determine the concentrations of weakly and strongly bound As, Fe, Mn and P in aquifer sediments in order to assess whether, and to what extent, As concentrations in surrounding groundwaters are associated with solid phase concentrations and other plausibly relevant groundwater/sediment parameters, such as pH, *Eh*, mean grain size (MGS) and solid phase arsenic speciation. The methods, results and interpretation reported in this paper expand upon those briefly outlined previously (Casanueva-Marenco et al., 2016).

2. Methods and materials

2.1. Field study area

The study area is located between the Mekong and Bassac River southeast of Phnom Penh, Cambodia, in northern Kandal Province (Fig. 1). This area has been the subject of extensive and ongoing research efforts on arsenic (bio)geochemistry, particularly given the generally very high concentrations of geogenic groundwater As (Polya et al., 2003, 2005; Charlet and Polya, 2006; Tamura et al., 2007; Benner et al., 2008; Kocar et al., 2008; Papacostas et al., 2008; Polizzotto et al., 2008; Rowland et al., 2008; van Dongen et al., 2008; Polya and Charlet, 2009; Lawson et al., 2013; Richards et al., 2015; Stuckey et al., 2015a,b; Lawson et al., 2016; Magnone et al., 2017; Richards et al., 2017a,b). A detailed description of the field area including site schematic was published previously (Richards et al., 2017a). Two contrasting transects broadly oriented parallel to the inferred direction of major groundwater flow were studied, viz., a clay-dominated transect, "T-Clay", located on floodplain deposits (sampling sites LR10, LR11, LR12, LR13 and LR14), and a sand-dominated transect, "T-Sand", located on scroll bar deposits of former river channels (sampling sites LR01, LR02, LR03, LR04, LR05, LR16, LR07, LR08 and LR09) (Magnone et al., 2017; Richards et al., 2017a). Throughout the study area, the thickness of a surficial clay layer varies significantly (from approximately 0–25 m in thickness), with T-Clay generally having more continuous and clay-dominated lithology than T-Sand (Uhlemann et al., 2017).

2.2. Sediment and groundwater sampling and sample pre-treatment

The installation of boreholes and sediment sample collection was carried out using manual rotary drilling between November 2013 and February 2014 along T-Sand and T-Clay using methods previously described (Richards et al., 2015, 2017a). Wet sediment cores were collected at target intervals of each three meters of depth using a locally-designed stainless steel sampler during drilling. Sediment subsamples for extractions and total organic carbon (TOC), total carbon (TC) and total nitrogen (TN) analysis (Magnone et al., 2017) were placed in an aluminium foil envelope that had been pre-furnaced to 430 °C (to minimize trace contamination) and placed in a zip seal polythene bag stored anaerobically. All cores for extractions and TOC/TC/TN analysis were stored frozen and transported to the University of Manchester for further analysis at the

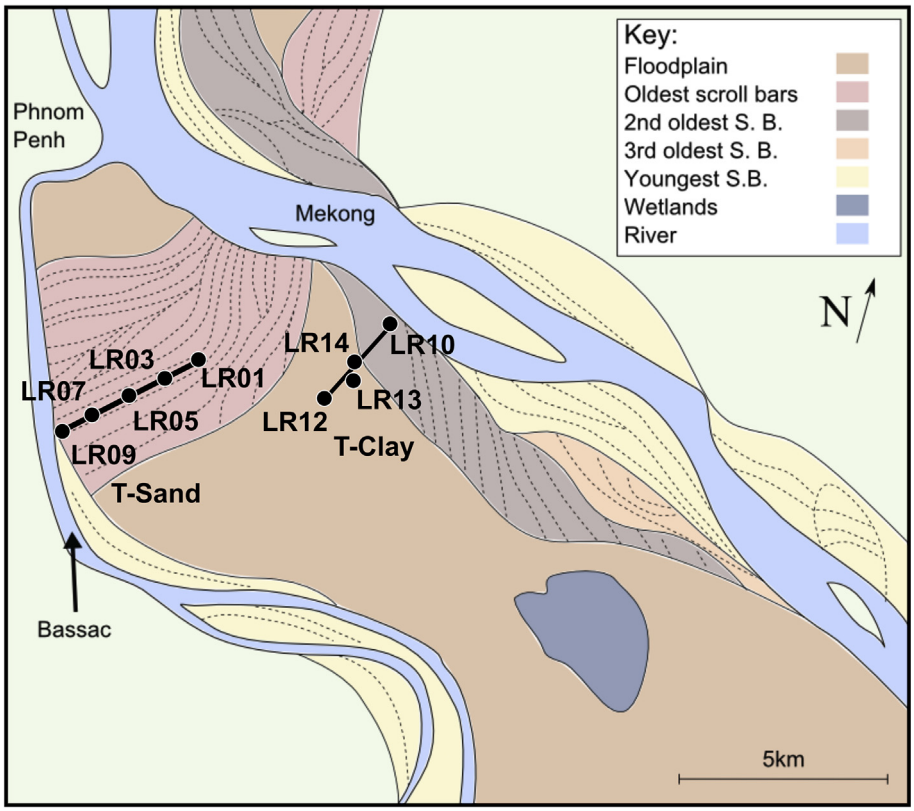

Figure 1. Site map showing location of transects, T-Sand and T-Clay, and of individual boreholes mentioned in the text. From Magnone et al. (2017) under terms of an open access CC-BY license, details of which may be found at http://creativecommons.org/licenses/by/4.0/.

Manchester Analytical Geochemistry Unit (MAGU). Sediment subsamples for particle size analysis were stored refrigerated in polyethylene bags until further analysis.

Groundwater samples were taken from the flushed and developed wells (Richards et al., 2015), screened over approximately 1 m at depths ranging from 6 to 45 m during pre- and post-monsoon sampling seasons in 2014 using methods previously described (Richards et al., 2017a). In brief, groundwater pH and *Eh* were measured *in-situ* using a multimeter (Professional Plus Series Portable Multimeter, YSI) with compatible sensors and a flow cell (all YSI). Subsamples of groundwater for analysis of groundwater As (As_{GW}), Fe (Fe_{GW}) and Mn (Mn_{GW}), amongst other analytes, were filtered (0.45 μm cellulose and polypropylene syringe filters, Minisart RC, UK), acidified to pH < 2 (trace grade nitric acid, BDH Aristar, VWR, UK), and refrigerated prior to analysis at MAGU (Richards et al., 2017a). The groundwater data presented here are medians of the two sampling seasons given the seasonal fluctuations in groundwater geochemistry (Richards et al., 2017a). Full inorganic characterisation of the groundwater, including specific data for each sampling season, is provided elsewhere (Richards et al., 2017a) as is an account of ^{3}He-^{3}H based model recharge rates (Richards et al., 2017b). The dataset presented in this manuscript is a subset where data were available to pair groundwater analysis with the corresponding analysis of sediments collected from the same sites and approximate depths.

2.3. Analytical methods

2.3.1. Sediment extraction procedures and analysis

Two separate single extraction procedures were applied in order to assess: (i) weakly sorbed (and associated with carbonate phases) As ($As_{Sed,W}$), Fe ($Fe_{Sed,W}$), Mn ($Mn_{Sed,W}$) and P ($P_{Sed,W}$), using glacial acetic acid (CH_3COOH, $\geq$ 99.85%, Sigma Aldrich, Germany) and (ii) strongly bound As ($As_{Sed,S}$), Fe ($Fe_{Sed,S}$) and Mn ($Mn_{Sed,S}$) by sodium dihydrogen phosphate monohydrate ($NaH_2PO_4 \cdot H_2O$, EMSURE grade, Millipore Sigma, UK) solutions (Eiche et al., 2008; Casanueva-Marenco et al., 2016). Strongly bound P in the sediments was not determined due to the chemical nature of the extractant. Table 1 shows a brief summary of experimental conditions carried out at each sediment extraction. The extraction solution (Table 1) was added to 1 g (±1 mg) of wet sediment in 50 mL clean polypropylene centrifuge tubes. Sediments were weighed using an analytical scale (PS-100, Fisher Scientific, UK). The mixture was mechanically shaken (Stuart Orbital shaker SSM1, Bibby Scientific, UK) for either 16 or 24 h, depending on the extraction, at a speed of 150 rpm at room temperature (Table 1), avoiding delay between the addition of the extraction solution and the beginning of shaking. After shaking, tubes were centrifuged (MSE Mistral 1000 Centrifuge, Sanyo, UK) at 2700 rpm for 20 min to facilitate the separation between phases and subsequent extraction of the supernatant liquid into a clean centrifuge tube. The tube containing supernatant was stored in a refrigerator at approximately 4 °C until analysis. Due to the nature of the NaH_2PO_4 extraction solution, final samples were diluted (by a factor of 20), and acidified with HNO_3 (1%, Suprapur, Merck, Germany) before analysis. Analysis of As in sediment extracts and groundwater (Richards et al., 2017a) was performed using inductively coupled plasma mass spectrometry (ICP-MS, Agilent 7500cx); and Fe, Mn and P using inductively coupled plasma atomic emission spectrometer (ICP-AES, Perkin-Elmer Optima 5300 dual view), both located in a clean laboratory environment (Class 1000) at MAGU. Widely-used extraction procedures (e.g. modified after Ure et al., 1993; Keon et al., 2001; Eiche et al., 2008) were selected to facilitate comparison with other work.

Table 1
Sediment extraction procedures used for trace metal assessment (modified after Ure et al., 1993; Keon et al., 2001; Eiche et al., 2008). Room temperature (RT) in the analytical facilities was approximately 18–20 °C.

Sediment fraction	Extractant	Conditions
Weakly Bound ($As_{Sed,W}$, $Fe_{Sed,W}$, $Mn_{Sed,W}$, $P_{Sed,W}$)	40 mL of 0.11 M CH_3COOH	Shake 16 h at RT Centrifuge at 2700 rpm
Strongly Bound ($As_{Sed,S}$, $Fe_{Sed,S}$, $Mn_{Sed,S}$)	20 mL of 0.5 M NaH_2PO_4 (adjusted at pH 5 with NaOH)	Shake 24 h at RT Centrifuge at 2700 rpm Dilution and acidification (1%)

Wet sediment was used for chemical extractions because dried sediments have been shown to over-release bound As compared to naturally wet samples and consequently do not accurately represent natural environmental conditions (Anawar et al., 2010). Explicit corrections for the variation in sediment moisture content were not made, however moisture content typically ranged from around 6% to >30%, with clay-dominant samples of relatively low mean grain size (MGS) typically having higher moisture content than sand-dominant samples with higher MGS and lower moisture content.

2.3.2. Sedimentary TOC, TC, TN and grain size determinations

Sedimentary TOC, TC and TN were measured using an elemental analyser (Vario EL Cube, Elementar) located in the Faculty of Life Sciences, University of Manchester (Magnone et al., 2017). In brief, sediments were freeze dried and ground, and subsamples for TC and TN (approximately 20 mg) were rolled into balls prior to analysis in triplicate. Subsamples for TOC and TN were prepared and measured using the capsule method as previously described (Brodie et al., 2011). In brief, approximately 20 mg of powdered sample was weighed into silver boats, mixed with 10 μL of deionised water and heated to 50 °C. HCl (analytical reagent grade, Fisher Brand, UK) was added in stepwise intervals (10, 20, 30, 50, 100 μL) to the heated silver boat. After the addition of the final aliquot the sample was dried and rolled into a ball for analysis (Brodie et al., 2011). Values of TN measured with TC and with TOC were compared to assess the influence of acidification. In the case that TOC exceeded TC but was within the range of analytical error, TOC was assumed to be equal to TC. Sediment particle size analysis was conducted on dried and sieved (<2 mm) subsamples using laser diffraction as previously described (Richards et al., 2017a). Reported here is the mean grain size (MGS) as defined by the Folk and Ward method and determined using the Gradistat_v8 statistics package (Blott and Pye, 2001).

2.4. Quality assurance and quality control (QA/QC)

Milli-Q deionised water (18.2 MΩ cm at 25 °C, Milli-Q Plus, Millipore, USA) was used for the preparation of all solutions and dilutions. All laboratory glassware was washed with Micro-90 laboratory soap (Sigma-Aldrich, UK) and rinsed with Milli-Q water to prevent contamination when measuring metal(loid)s at trace concentrations. Centrifuge tubes and pipette tips were soaked overnight in a 2 M nitric acidbath (Suprapur grade, Merck, Germany), rinsed thoroughly with Milli-Q water and air dried in within the fume hood to avoid possible contamination. When dried, the materials were sealed and kept in polyethylene bags until use.

In both extraction procedures, procedural blank samples (with no sediment) were carried out following the same protocol as for sediment samples. For the extraction experiments, each sediment sample was processed in duplicate, and ICP-MS and ICP-AES analysis was conducted in triplicate to assess the precision of the methods. Matrix-matched calibration standards diluted from As, Fe, Mn and P single element standard solutions (1000 mg/L, Aristar, VWR, UK) were run every ten samples. Using the reagent blank, limits of detection (LoD) and quantification (LoQ) were determined for each extractant solution and for each analyte with the corresponding technique (Table 2). No suitable matrix-matched certified reference material (CRM) was available for this procedure.

The QA/QC for groundwater measurements and analyses, including the use of CRMs and inverse variance weighted first order linear calibration models (Miller and Miller, 2010; Polya et al., 2017) are discussed in detail elsewhere (Polya et al., 2017; Polya and Watts, 2017; Richards et al., 2017a). For sedimentary TOC measurements, soil standards of varying carbon content (Elemental Microanalysis Cat. Nos. B2152, B2153, B2178 and B2150) were included for data quality analysis and further samples ($n = 9$) were sent to UKAS-accredited Elemental Microanalysis for external validation (Magnone et al., 2017).

2.5. Multiple linear regression (MLR) analysis

Multiple linear regression (MLR) analysis was conducted to quantitatively assess the importance of various measured parameters (*Eh*, pH, Fe_{GW}, $As_{Sed,W}$, $Fe_{Sed,W}$, $As_{Sed,S}$, $Fe_{Sed,S}$, TOC and MGS) in controlling As_{GW}. As_{GW} (μM) was modelled from selected variables measured: pH, *Eh* (mV), Fe_{GW} (μM), $As_{Sed,W}$ (μg/g), $Fe_{Sed,W}$ (μg/g), $As_{Sed,S}$ (μg/g), $Fe_{Sed,S}$ (μg/g), TOC (% w/w) and MGS (μm). The null hypothesis (H_0) was that there is no relationship between As_{GW} and a given variable, and T-values, p-values and the F-statistic were used to assess whether H_0 could be rejected at the 95% confidence level. The predictive MLR equation (Eq. (1)) was

$$As_{GW,\ Modelled} = m_1x_1 + m_2x_2 + \ldots + m_nx_n + c \quad (1)$$

where m is the coefficient of parameter n, x is the value of subscripted variable n and c is the residual. Unrefined models contained each of the potentially explanatory variables listed and refined models contained only those parameters which were statistically significant at the 95% confidence level. MLR offers the advantage over single correlation statistics because multiple possible explanatory variables can be considered together in MLR. The F-Statistic is reported as F (regression df, residual df) = value; F significance = value, where df = degrees of freedom, and standard regression statistics are reported as t(df) = t value; $p = p$ value. All statistical analyses were completed using the statistical packages in OriginPro 2015 and/or the Data Analysis tool pack of Microsoft Excel 2010.

Table 2
Limit of detection (LoD) and quantification (LoQ) for As, Fe, Mn and P in different matrices. CH_3COOH was used to as the extractant for weakly bound analytes and NaH_2PO_4 as the extractant for strongly sorbed analytes; As was analysed with ICP-MS and Fe, Mn and P with ICP-AES.

Matrix	CH_3COOH (0.11 M)				NaH_2PO_4 (0.5 M)		
Analyte	As (μg/L)	Fe (mg/L)	Mn (mg/L)	P (mg/L)	As (μg/L)	Fe (mg/L)	Mn (mg/L)
LoD	0.01	0.02	0.01	0.01	0.14	0.04	0.01
LoQ	0.03	0.08	0.05	0.04	0.48	0.12	0.02

Table 3
Groundwater and paired sediment data from T-Sand and T-Clay transects. The subscripts GW, Sed,W and Sed,S refer to groundwater, weakly sorbed and strongly sorbed forms of the associated chemical component.

Site	Depth (m)[a]	Groundwater[b]					Sediment									
										Weakly sorbed				Strongly bound		
		pH	*Eh* (mV)	As_{GW} (μM)	Fe_{GW} (μM)	Mn_{GW} (μM)	MGS[c] (μm)	TOC[d] (%)	Moisture content (%)	$As_{Sed,W}$ (μg/g)	$Fe_{Sed,W}$ (μg/g)	$Mn_{Sed,W}$ (μg/g)	$P_{Sed,W}$ (μg/g)	$As_{Sed,S}$ (μg/g)	$Fe_{Sed,S}$ (μg/g)	$Mn_{Sed,S}$ (μg/g)
T-Sand																
LR01	6	6.8	0	0.2	3	46	40	1.20	24	0.24	1700	178	2.3	1.3	61	34
	9	6.9	−143	2.7	215	26	66	0.30	19	0.21	1150	71	2.6	0.6	50	21
	15	6.9	−103	0.9	66	15	118	0.10	20	0.13	526	57	1.3	0.8	33	27
	21	6.9	−108	2.2	176	8	232	0.08	17	0.04	209	38	n/d	0.6	32	14
	30	7.0	−138	7.3	162	11	60	0.07	6	0.14	568	147	11	0.7	31	23
LR02	15	6.9	−109	1.7	64	11	114	0.22	12	0.21	245	213	n/d	1.4	31	101
	30 (27)	7.1	−94	8.6	128	12	1070	0.07	8	0.07	57	114	0.9	0.8	28	21
LR03	15	7.0	−135	1.2	65	13	123	0.04	16	0.12	184	141	0.7	1.6	26	63
LR04	15 (12)	7.0	−83	2.2	76	18	85	0.21	27	0.07	252	58	3.3	0.9	29	43
	30	7.2	−112	5.4	82	12	21	0.74	27	0.25	803	57	5.5	1.2	64	14
LR05	6	6.7	−66	0.3	22	84	19	0.77	30	0.10	1040	164	1.6	1.0	43	41
	9	7.1	−166	2.9	89	57	59	0.37	18	0.22	1180	95	3.3	1.1	45	21
	15	6.9	−150	3.1	505	31	198	0.10	18	0.08	394	29	1.5	0.7	34	14
	21	7.2	−147	7.3	127	11	125	0.06	13	0.14	383	58	1.1	0.9	30	20
	30	7.1	−153	8.6	105	6	9	1.19	29	0.19	268	6	7.0	1.8	30	4
LR16	15	6.8	−81	5.2	417	11	n/a	0.41	20	0.10	660	230	1.3	0.7	29	28
	30	6.8	−40	1.7	16	3	n/a	0.90	23	0.11	492	63	1.6	1.5	35	9
LR07	15	6.7	−33	0.7	182	13	123	0.15	17	0.12	807	64	2.8	0.6	38	18
	30	7.0	−87	8.1	216	5	45	0.61	17	0.10	474	80	1.2	0.8	29	18
LR08	30	6.9	−93	4.2	150	4	171	0.12	18	0.09	913	126	1.3	0.7	29	26
LR09	6	6.9	−70	0.1	17	22	22	1.27	30	0.26	1230	180	4.9	1.3	31	16
	9	6.8	−139	2.3	181	34	45	0.54	23	0.23	964	86	2.4	1.1	30	18
	21	7.0	−131	8.3	223	10	88	0.14	22	0.12	698	53	2.7	0.7	39	17
	30	7.2	−153	10.4	153	7	548	0.01	6	0.09	124	58	1.4	0.9	27	6
	45	7.3	−105	0.2	5	27	299	0.06	18	0.15	333	50	0.8	2.5	31	17
T-Clay																
LR10	6	6.9	−11	1.1	0	2	81	0.17	19	0.92	597	155	2.2	3.7	26	51
	9	7.0	−106	4.1	136	20	92	0.19	17	0.98	132	79	4.1	8.7	28	39
	15	7.0	−121	5.8	193	10	245	0.18	18	0.15	446	57	1.8	1.6	31	19
	21	7.5	−155	13.7	56	40	178	0.09	16	0.20	619	76	1.2	1.6	29	24
	24 (30)	7.5	−125	5.8	25	20	244	0.10	19	0.43	545	99	2.2	1.5	31	22
LR12	30	6.9	−33	5.9	84	20	100	0.72	n/a	0.17	590	145	4.1	1.4	2.2	28
LR13	30	6.9	−53	6.1	77	4	n/a	1.07	26	0.26	559	217	1.1	4.1	26	29
LR14	6	7.1	18	0.0	1	24	6	0.15	25	0.00	2	7	n/d	0.7	8	9
	9	6.8	4	0.1	15	13	12	1.97	31	0.22	272	35	2.8	1.6	27	8
	15	6.9	−53	0.3	37	10	41	1.25	38	0.39	234	6	4.9	4.0	25	2
	21	6.9	−50	2.6	144	3	57	0.26	20	0.43	588	70	5.8	1.6	25	14
	30	6.7	−62	3.8	97	4	35	0.47	23	0.11	556	73	2.4	1.4	30	13

[a] Depth typically refers to the depth of both water and corresponding sediment samples; in the case where a depth is reported as XX (YY) the XX refers to the depth of the water and (YY) is the depth of the sediment samples (differences were due to sediment sampling challenges at some sites).
[b] Groundwater characteristics are reported as the *median* value of pre- and post-monsoon sampling campaigns (full data for individual campaigns including errors are reported in Richards et al., 2017a; note samples LR01-6, LR16-15 and LR16-30 were only sampled post-monsoon).
[c] Mean grain size (MGS, Folk and Ward method; Richards et al., 2017a); n/a indicates data not available and n/d not detected.
[d] Total organic carbon (TOC) was previously reported (Magnone et al., 2017). A site schematic and map are provided elsewhere (Richards et al., 2017a). No strongly bound P is reported due to the nature of the extractant.

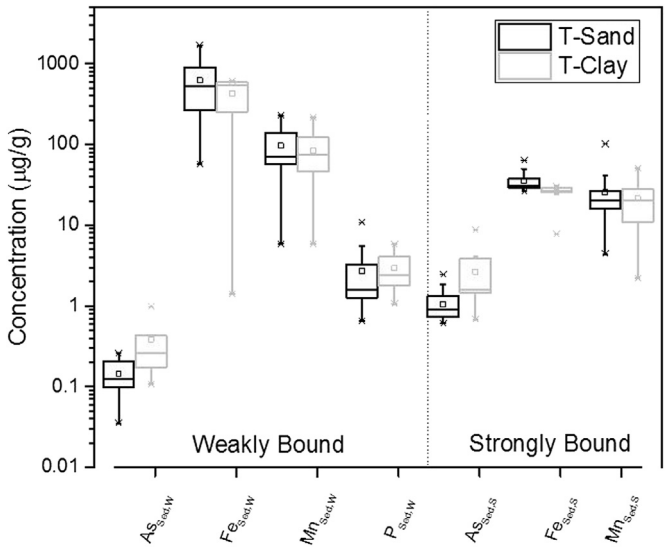

Figure 2. Box chart representing summary statistics on a logarithmic scale of sedimentary extraction data for T-Sand (black boxes) and T-Clay (grey boxes). The subscripts Sed,W and Sed,S refer to weakly sorbed and strongly sorbed forms of the associated chemical component. Boxes represent the 25% and 75% range; the line within the box represents the median; the square represents the mean; the x represents the 1% and 99% range; and the straight lines indicate the maximum and minimum.

3. Results and discussion

3.1. Groundwater and sediment data

The groundwater and sediment characteristics are shown in Table 3. The pH and *Eh* values of groundwater ranged from 6.7 to 7.5 (median: 6.9) and from −170 to 18 mV (median: −103 mV). As_{GW} ranged from 0.11 to 10.4 µM for T-Sand and 0.03 to 13.7 µM for T-Clay, generally increasing with depth, positively associated with Fe_{GW}, and consistent with As mobilization via reductive dissolution of Fe (hydr)oxides (Richards et al., 2017a). Further details on the characterization of inorganic aqueous geochemistry are provided elsewhere (Richards et al., 2017a).

In sediments (Fig. 2 and Table 3), strongly bound $As_{Sed,S}$ (0.6 − 2.5 µg/g for T-Sand; 0.7 − 8.7 for T-Clay) was higher than weakly bound $As_{Sed,W}$ (0.04 − 0.26 µg/g for T-Sand; <DL − 0.98 µg/g for T-Clay). This perhaps reflects the similar geochemical behaviour of AsO_4^{3-} and PO_4^{3-}, leading to sorption of arsenate and phosphate (Feng et al., 2013; Meng et al., 2017). On the other hand, weakly bound $Fe_{Sed,W}$ (57–1700 µg/g for T-Sand; 1–620 µg/g for T-Clay) and $Mn_{Sed,W}$ (6 − 230 µg/g for T-Sand; 6–220 µg/g for T-Clay) were higher than strongly bound $Fe_{Sed,S}$ (26 − 64 µg/g for T-Sand; 8 − 31 µg/g for T-Clay) and $Mn_{Sed,S}$ (4 − 100 µg/g for T-Sand; 2–50 µg/g for T-Clay). This suggests the high tendency of these elements (e.g. Fe and Mn) to be associated with the exchangeable and carbonate fraction of the sediment instead of the strongly or specifically adsorbed As. Although slight differences in ranges were noted between T-Sand and T-Clay, the general trends between analytes was consistent between the two transects. For example, $As_{Sed,S}$ was always higher than $As_{Sed,W}$ in both transects, even though the concentrations of both $As_{Sed,S}$ and $As_{Sed,W}$ were higher in T-Clay than in T-Sand.

3.2. Factors controlling assorption processes

There is an overall statistically significant positive correlation between As_{GW} and pH (Fig. 3A; $R^2_{adj} = 0.31$; $t(71) = 5.8$, $p < 0.05$) as well as a negative correlation between As_{GW} and *Eh* (Fig. 3B; $R^2_{adj} = 0.19$; $t(71) = -4.2$, $p < 0.05$). The highest As_{GW} is observed in relatively high pH and highly reducing conditions. These overall relationships relate to the entire dataset across the entire field area; however T-Sand and T-Clay subsets show distinct behaviour. For example, many T-Clay samples fall within the lower pH range (with the exception of 4 samples at distinctly high pH) and on the higher range of *Eh*. Conversely, most T-Sand samples fall between pH 6.9 and 7.2 and are strongly reducing in the low *Eh* range. There appears to be a particularly strong relationship between As_{GW} and *Eh* in the strongly reducing groundwaters; a correlation which

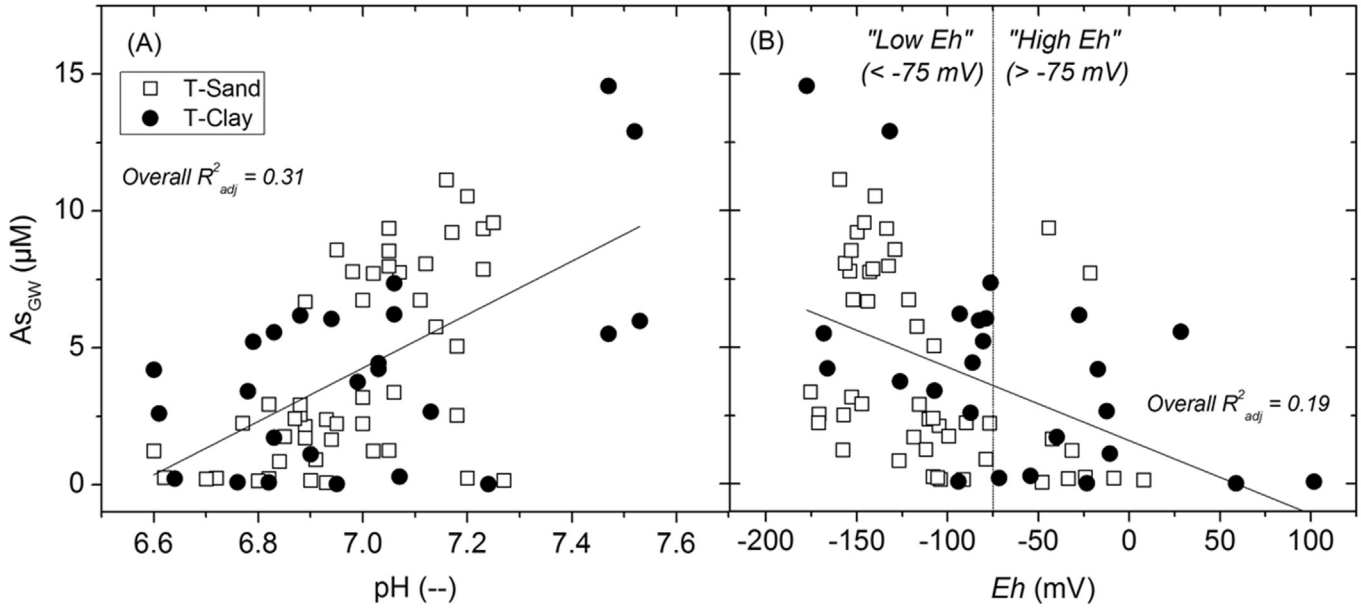

Figure 3. Groundwater arsenic (As_{GW}) in T-Sand (open squares) and T-Clay (filled circles) during pre- and post-monsoon sampling seasons as a function of (A) pH and of (B) *Eh* with "Low *Eh*" and "High *Eh*" subsets used later in this manuscript indicated by the dashed line. Most As_{GW} concentrations far exceed the World Health Organization (WHO) provisional drinkingwater guideline of 0.13 µM (10 µg L^{-1}; World Health Organization, 2011; Richards et al., 2017a).

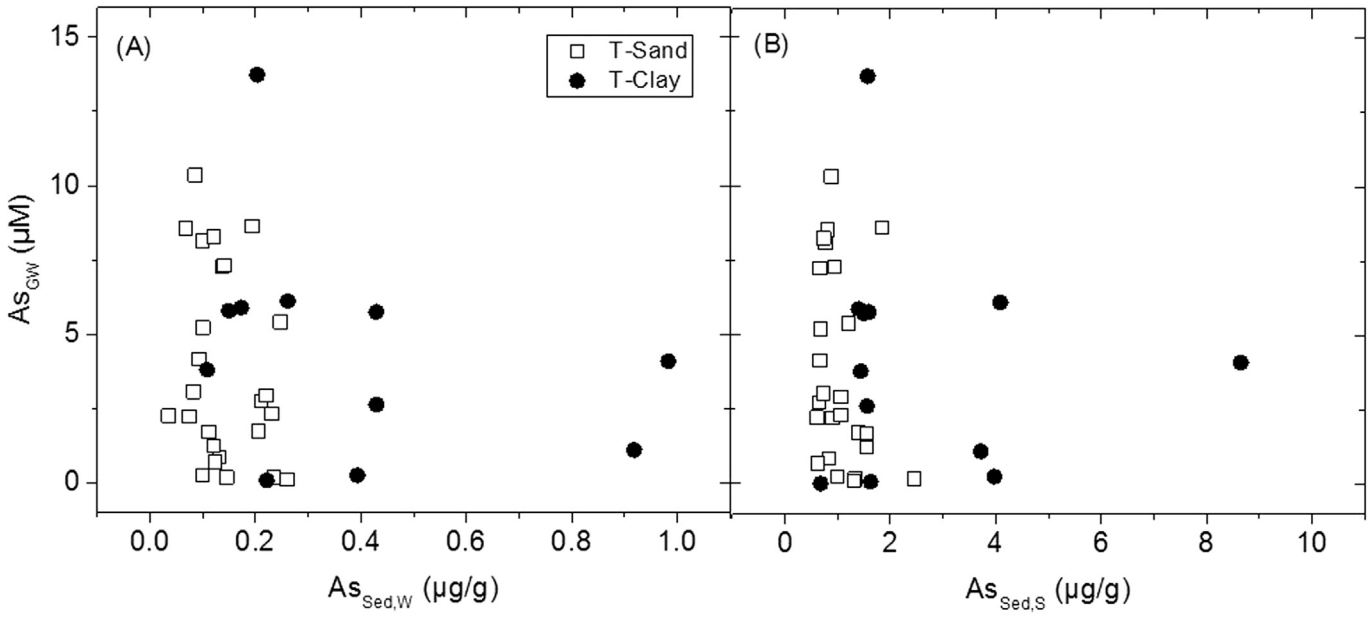

Figure 4. Groundwater arsenic (As_{GW}) in T-Sand (open squares) and T-Clay (filled circles) versus corresponding weakly bound sedimentary arsenic ($As_{Sed,W}$) and strongly bound sedimentary arsenic ($As_{Sed,S}$).

becomes weaker as *Eh* increases. These "envelope" observations provide justification for splitting the data into groupings for further interpretation: (i) by transect (T-Sand versus T-Clay) and (ii) by *Eh* ("low *Eh*"<−75 mV versus "high *Eh*">−75 mV), noting this distinction is a simplification of the broad distribution in *Eh* naturally encountered in such groundwaters.

The direct relationship between As_{GW} and either $As_{Sed,S}$ or $As_{Sed,W}$ is poor (Fig. 4), highlighting that the controls on As mobility are very complex and cannot be approximated by simply considering the corresponding bound sedimentary composition, and that conversely, sampled water chemistry may not be representative of key biogeochemical processes resulting in arsenic release. This is an important observation and suggests that (partial) re-equilibrium processes may be re-setting groundwater As concentrations along groundwater flow paths. This observation is particularly apparent in T-Clay, where samples containing by far the highest $As_{Sed,S}$ and/or $As_{Sed,W}$ do not necessarily correspond to the highest groundwater As concentrations. This could be plausibly attributed, in part, to sorption/desorption processes arising particularly because of higher surface area and lower permeabilities associated with clay sediments as well as other biogeochemical controls such as seasonally-shifting redox conditions, pH dependent dissolution of carbonates and the nature of the associated surface-derived or sedimentary OM (Lawson et al., 2013, 2016; Stuckey et al., 2016; Magnone et al., 2017; Richards et al., 2017a). $As_{Sed,S}$ and $As_{Sed,W}$ are significantly correlated for T-Clay (Fig. 5, $R^2_{adj} = 0.54$; $t(9) = 3.6$, $p < 0.05$), although this relationship does not hold for T-Sand. There are distinct differences between T-Sand and T-Clay – for example, $As_{Sed,W}$ and $As_{Sed,S}$ vary significantly more in T-Clay than they do in T-Sand, although this is not necessarily reflected in groundwater concentrations. This contrasting behaviour has important implications on interpreting the degree to which the nature of key biogeochemical processes can be accurately deduced from sampled water chemistry and warrants examination in greater detail.

The relationship between As_{GW} and $Fe_{Sed,W}$ (Fig. 6A) is statistically significant for T-Sand ($R^2_{adj} = 0.14$; $t(23) = -2.2$, $p < 0.05$) but not T-Clay ($R^2_{adj} = 0.23$; $t(10) = 2.1$, $p > 0.05$) which further highlights that the controls on As_{GW} are different in each transect. The negative correlation between As_{GW} and $Fe_{Sed,W}$ on T-Sand suggests that dissolved As_{GW} may be sequestered by sorption/re-absorption onto Fe minerals of the sediments in this transect. In T-Clay this correlation is not statistically significant which suggests a different process is dominant in this transect. The distinction by transect appears to be stronger than simple distinctions with *Eh* (Fig. 6B), where there is not a significant correlation between As_{GW} and $Fe_{Sed,W}$ for either the high *Eh* or low *Eh* group. Interestingly, this observation is consistent with the positive correlation observed between $As_{Sed,W}$ and $Fe_{Sed,W}$ in T-Sand (Fig. 7A, $R^2_{adj} = 0.36$; $t(23) = 3.8$, $p < 0.05$), which is suggestive of the importance of sorption of aqueous As(III) to Fe-bearing mineral phases in this transect. T-Sand was the only grouping where a significant relationship between $As_{Sed,W}$ and $Fe_{Sed,W}$ was observed (Fig. 7).

There is a negative correlation between MGS and $As_{Sed,W}$ on T-Sand (Fig. 8A, $R^2_{adj} = 0.18$; $t(21) = -2.4$, $p < 0.05$), indicating that

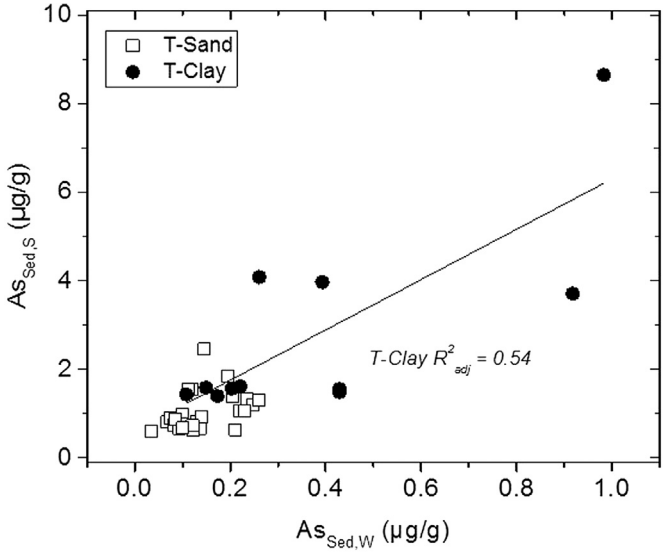

Figure 5. Strongly bound sedimentary arsenic ($As_{Sed,S}$) versus weakly bound sedimentary arsenic ($As_{Sed,W}$) for T-Sand (open squares) and T-Clay (filled squares) showing a statistically significant linear correlation for T-Clay.

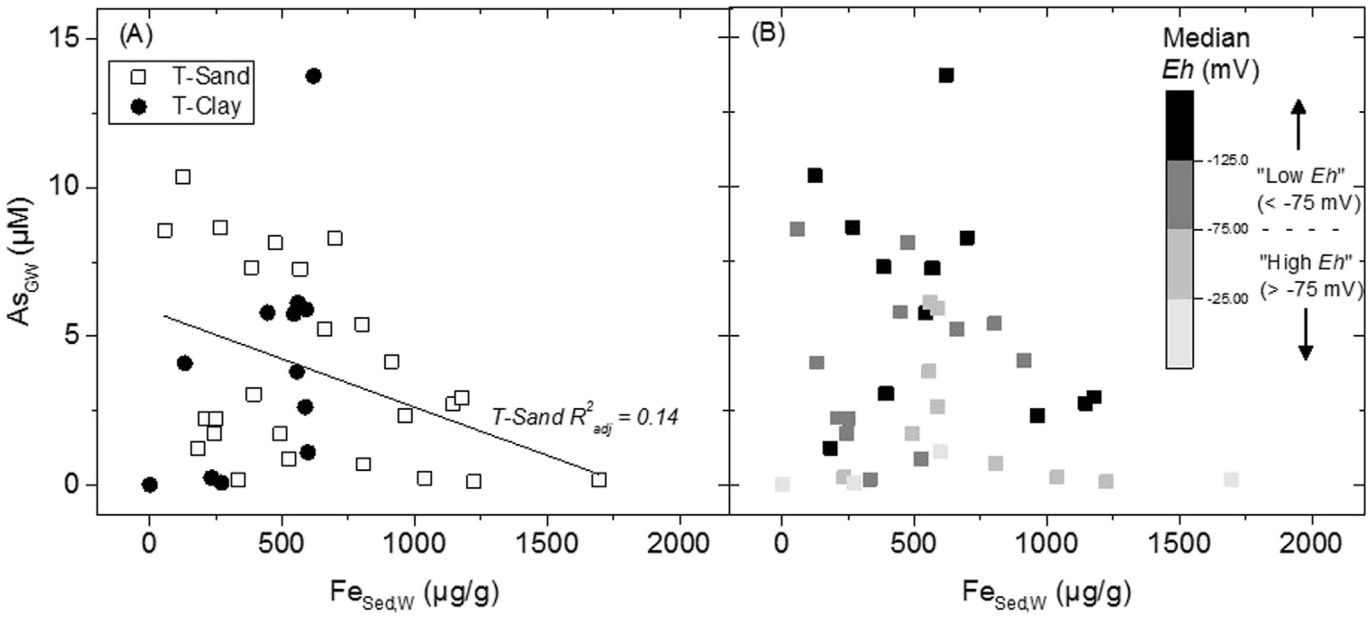

Figure 6. Groundwater arsenic (As_{GW}) (µM) against corresponding weakly sorbed sedimentary iron ($Fe_{Sed,W}$) (µg/g) grouped according to (A) transect as indicated by symbol shape; and (B) groundwater *Eh* as indicated by grey scale. Groundwater *Eh* and As_{GW} are reported as the median of pre- and post-monsoon measurements. Correlations are only shown where significant at the 0.05 level (e.g. the only statistically significant correlation is on T-Sand).

finer sediments contain more sorbed As which is expected given the greater specific surface areas of such fine sediments (and thus higher sorption capacity for most metals) (Duan et al., 2013; Li et al., 2015). This relationship does not hold on T-Clay. However, on T-Clay, there is a strong negative correlation between *Eh* and MGS (Fig. 8C, $R^2_{adj} = 0.60$; $t(21) = -4.0$, $p < 0.05$), which means that the groundwater hosted in the finer sediments is much less reducing than in the higher MGS sediments. In this case, even though the finer sediments are likely to have higher sorption capacity and contain more weakly sorbed As (because of the higher specific surface area of the fine grains), the redox conditions might not be suitable (e.g. not sufficiently reducing) for As to be mobilized. This could offer a possible explanation for why the relationship between MGS and $As_{Sed,W}$ is not significant on T-Clay. There are not significant correlations for either $As_{Sed,W}$ nor *Eh* with MGS for the *Eh* groupings (Fig. 8B and D, respectively).

Note that the classifications of "T-Sand" and "T-Clay" are simplified groupings and both borehole logs and separate electrical resistivity tomography studies (Uhlemann et al., 2017) indicate that there is considerable heterogeneity in these transects; for example

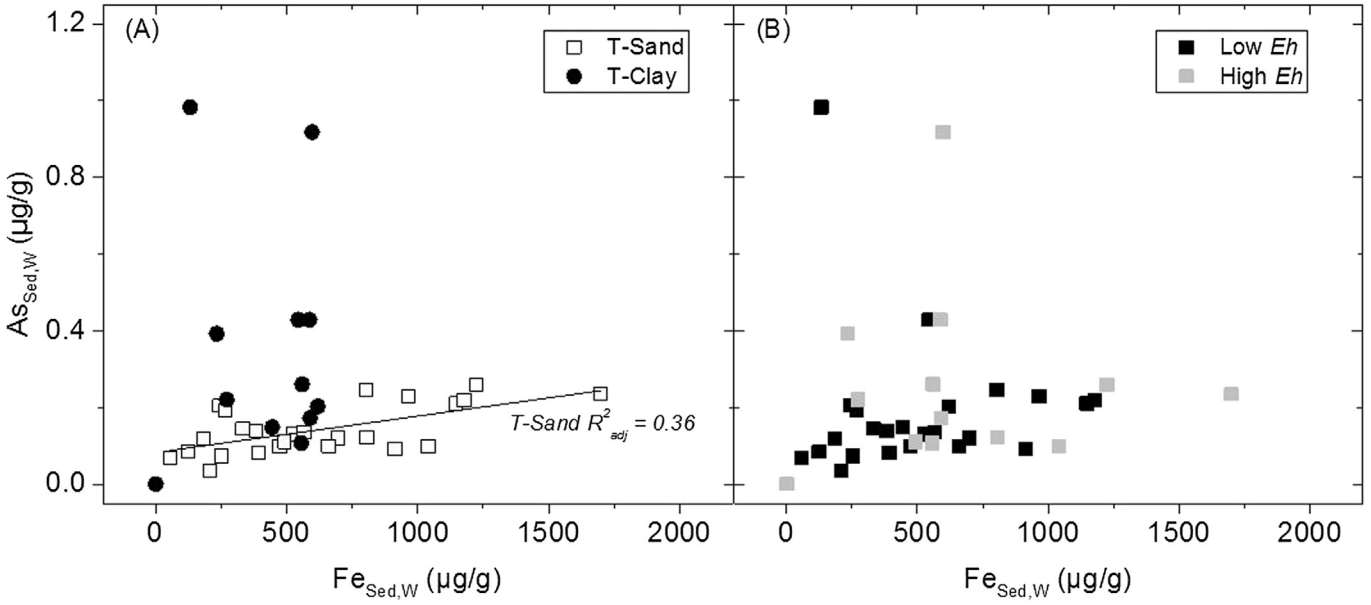

Figure 7. Weakly sorbed sedimentary arsenic ($As_{Sed,W}$) (µg/g) versus weakly sorbed sedimentary iron ($Fe_{Sed,W}$) (µg/g) grouped according to (A) transect as indicated by symbol shape; and (B) groundwater *Eh* as indicated by symbol colour. Correlations are only shown where significant at the 0.05 level (e.g. the only statistically significant correlation is on T-Sand).

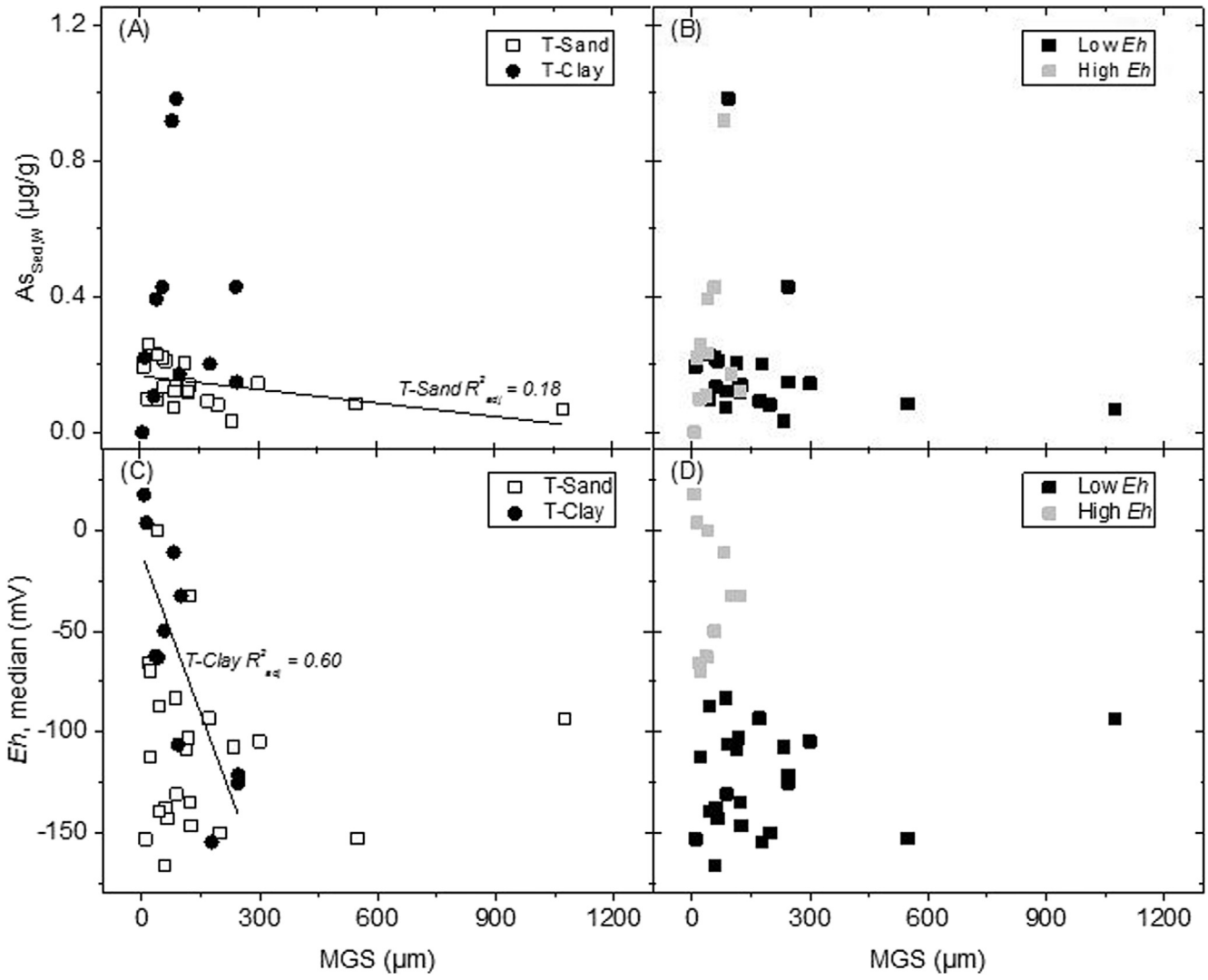

Figure 8. Weakly sorbed sedimentary arsenic ($As_{Sed,W}$) (µg/g) versus sedimentary mean grain size (MGS) (A and B) and *Eh* versus MGS (C and D) grouped according to (A and C) transect as indicated by symbol shape; and (B and D) groundwater *Eh* as indicated by symbol colour. Correlations within groupings are only shown where significant at the 0.05 level.

although T-Clay generally contains higher clay content, there are isolated and localized exceptions to this, for example at site LR10 which is very sandy (hence with higher MGS) despite being located on the clay-dominated transect. Similarly, there are samples containing clay, particularly at shallower depths, on T-Sand. Further, the use of MGS as a proxy to characterize the sediment grain size is a major simplification. In reality, grain sizes are distributed across sometimes a wide range of sizes (Fig. 9) and it would be expected that the different size fractions could all contribute in varying ways to these interactions. For example, a sample with high MGS may still have significant proportions of small, high surface area grains, all of which may contribute to the bulk observed behaviour.

On T-Sand, $As_{Sed,W}$ is correlated with sedimentary TOC (Fig. 10A, $R^2_{adj} = 0.30$; $t(23) = 3.4$, $p < 0.05$), this relationship being is largely 1st order linear with increases in TOC correlated to increases in $As_{Sed,W}$. However, on T-Clay, there appear to be two distinct trends, (i) a wide range of $As_{Sed,W}$ when TOC is less than approximately 0.25%, and (ii) at TOC levels above this cut-off (i.e. > 0.25%), $As_{Sed,W}$ varies with TOC in a very similar manner to what was observed on T-Sand. These patterns may indicate a degree of association of As-bearing Fe minerals to the sedimentary OM as observed elsewhere in soils (Kaiser and Guggenberger,

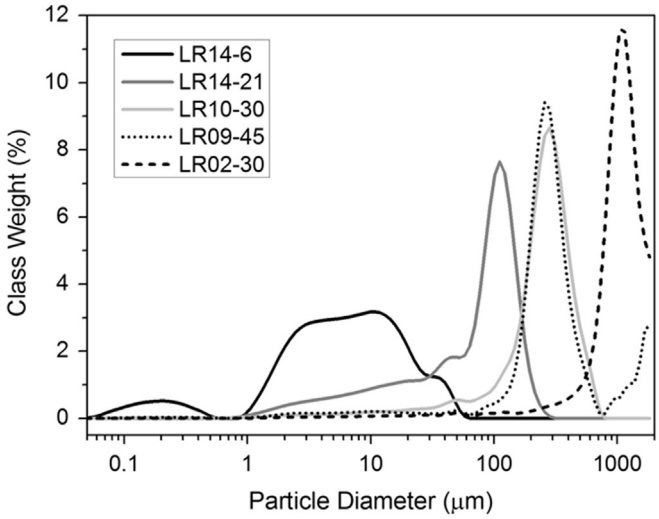

Figure 9. Distribution of sedimentary grain size for a range of samples on T-Clay (LR14-6, LR14-21 and LR10-30) (solid lines) and T-Sand (LR09-45 and LR02-30) (dashed lines).

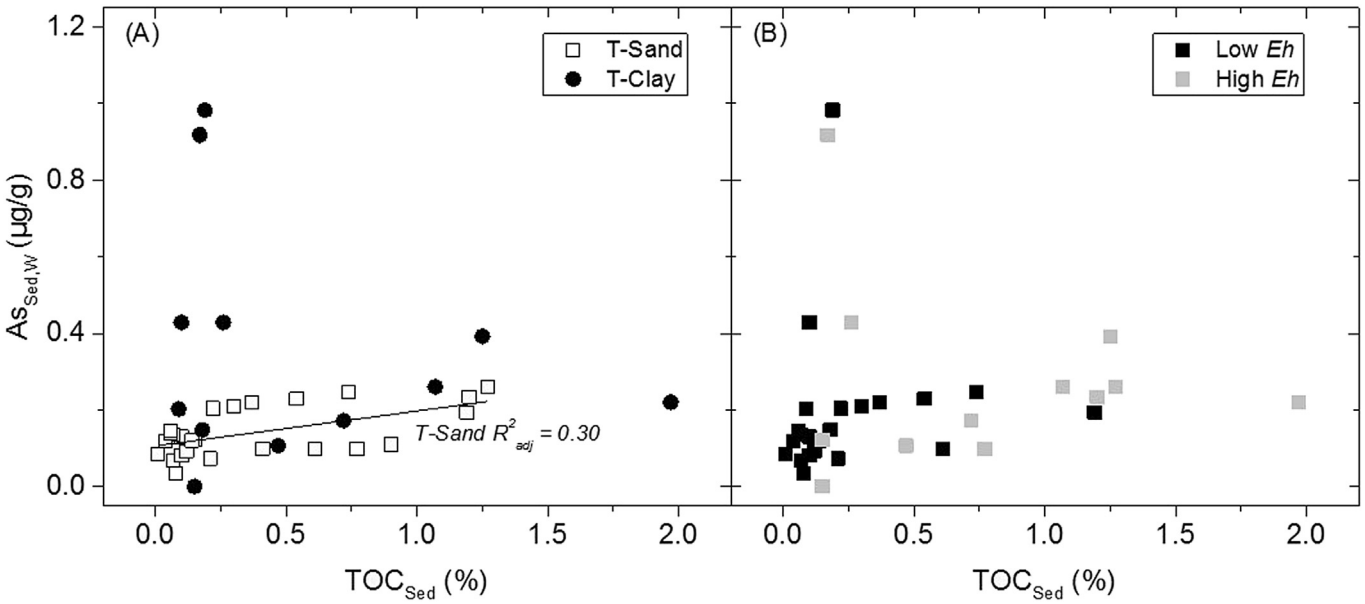

Figure 10. Weakly sorbed sedimentary arsenic ($As_{Sed,W}$) (µg/g) versus sedimentary total organic carbon (TOC_{sed}) (%) grouped according to (A) transect as indicated by symbol shape; and (B) groundwater *Eh* as indicated by symbol colour. Correlations are only shown where significant at the 0.05 level (e.g. the only statistically significant correlation is on T-Sand).

2000) and marine sediments (Vandenbroucke and Largeau, 2007; Lalonde et al., 2012; Johnson et al., 2015). The similarities become particularly apparent given the similar correlations with grainsize (Roy et al., 2013). It is plausible the plateauing observed in Fig. 10 is caused because As is sorbing to functional groups on the TOC surface in two scenarios: (i) when TOC is low (e.g.<0.25%) the sorption is high because the TOC contributes to the number of sorption sites and magnitude of surface area; however (ii) when TOC is relatively high (e.g. >0.25%) the TOC is mostly in the bulk phase and thus does not the availability of sorption sites for minerals might become comparatively limited.

3.3. Multiple linear regression (MLR) analysis

MLR was conducted to quantitatively assess the importance (or otherwise) of measured and potentially explanatory variables (*Eh*, pH, Fe_{GW}, $As_{Sed,W}$, $Fe_{Sed,W}$, $As_{Sed,S}$, $Fe_{Sed,S}$, TOC and MGS) in controlling As_{GW}. When MLR was conducted on the entire dataset using an unrefined model with all potentially explanatory variables, the correlation was relatively poor but statistically significant (Multiple $R = 0.74$; $F\,(9, 27) = 3.6$; F significance < 0.05) and the only statistically significant individual input was pH (Table 4A). A refined model of the entire dataset predicted As_{GW} using pH and

Table 4
Summary of MLR for arsenic in groundwater conducted on the (A) overall dataset and split by transect (B) T-Sand and (C) T-Clay. The table shows both an unrefined model with all variables and a refined model with only variables for which H_0 has been rejected at the 95% confidence level. The F-statistic is reported as F (regression df, residual df) = value, where df = degrees of freedom. Note the unrefined models use all of the same explanatory variables although the refined models may use different explanatory variables depending on statistical significance.

(A) Overall					(B) T-Sand					(C) T-Clay				
Unrefined	Estimate	Std. Error	*t* value	*P*-value	Unrefined	Estimate	Std. Error	*t* value	*P*-value	Unrefined	Estimate	Std. Error	*t* value	*P*-value
(Intercept)	−71.7	22.9	−3.1	<0.05	(Intercept)	−92.3	30.3	−3.1	<0.05	(Intercept)	−116	85.0	−1.4	0.31
pH	10.5	3.3	3.2	<0.05	pH	14.3	4.6	3.1	<0.05	pH	15.9	11.4	1.4	0.39
Eh (mV)	−0.01	0.01	−0.8	0.45	*Eh* (mV)	−0.004	0.02	−0.2	0.84	*Eh* (mV)	0.02	0.06	0.3	0.81
Fe_{GW} (µM)	0.01	0.01	2.0	0.05	Fe_{GW} (µM)	0.004	0.005	0.9	0.39	Fe_{GW} (µM)	0.02	0.03	0.6	0.63
$As_{Sed,W}$ (µg/g)	−1.5	4.2	−0.4	0.72	$As_{Sed,W}$ (µg/g)	0.2	13.0	0.0	0.99	$As_{Sed,W}$ (µg/g)	−10.2	7.3	−1.4	0.30
$Fe_{Sed,W}$ (µg/g)	0.0009	0.002	0.4	0.67	$Fe_{Sed,W}$ (µg/g)	−0.002	0.002	−1.1	0.28	$Fe_{Sed,W}$ (µg/g)	0.01	0.01	1.2	0.36
$As_{Sed,S}$ (µg/g)	0.2	0.6	0.3	0.77	$As_{Sed,S}$ (µg/g)	−4.5	1.5	−3.0	<0.05	$As_{Sed,S}$ (µg/g)	1.2	1.0	1.2	0.36
$Fe_{Sed,S}$ (µg/g)	−0.04	0.07	−0.5	0.60	$Fe_{Sed,S}$ (µg/g)	−0.02	0.06	−0.3	0.80	$Fe_{Sed,S}$ (µg/g)	0.32	0.6	0.58	0.63
TOC (%)	1.4	1.2	1.1	0.28	TOC (%)	4.1	1.7	2.5	<0.05	TOC (%)	−1.7	3.3	−0.5	0.65
MGS (µm)	0.004	0.003	1.3	0.21	MGS (µm)	0.002	0.002	0.9	0.39	MGS (µm)	−0.02	0.03	−0.8	0.53
Residual standard error = 2.7 (27 df)					Residual standard error = 2.1 (15 df)					Residual standard error = 2.5 (2 df)				
Multiple $R = 0.74$; $R^2 = 0.55$; Adjusted $R^2 = 0.40$					Multiple $R = 0.86$; $R^2 = 0.74$; Adjusted $R^2 = 0.59$					Multiple $R = 0.96$; $R^2 = 0.93$; Adjusted $R^2 = 0.59$				
F-statistic: $F\,(9, 27) = 3.6$; F significance < 0.05					F-statistic: $F\,(9,15) = 4.8$; F significance = < 0.05					F-statistic: $F\,(9,2) = 2.8$; F significance = 0.30				
Refined	Estimate	Std. Error	*t* value	*P*-value	Refined	Estimate	Std. Error	*t* value	*P*-value	Refined	Estimate	Std. Error	*t* value	*P*-value
(Intercept)	−78.2	15.3	−5.1	<0.05	(Intercept)	−96.3	20.6	−4.7	<0.05	(Intercept)	−73.5	14.0	−5.3	<0.05
pH	11.6	2.2	5.3	<0.05	pH	15.3	3.0	5.1	<0.05	pH	10.2	2.0	5.2	<0.05
Fe_{GW} (µM)	0.01	0.00	3.1	<0.05	$Fe_{Sed,W}$ (µg/g)	−0.003	0.001	−2.6	<0.05	$As_{Sed,W}$ (µg/g)	−10.4	2.8	−3.7	<0.05
–					$As_{Sed,S}$ (µg/g)	−5.5	1.1	−5.0	<0.05	$Fe_{Sed,W}$ (µg/g)	0.01	0.00	5.0	<0.05
–					TOC (%)	3.7	1.3	2.7	<0.05	$As_{Sed,S}$ (µg/g)	1.5	0.4	3.8	<0.05
Residual standard error = 2.5 (34 df)					Residual standard error = 1.9 (20df)					Residual standard error = 1.6 (7 df)				
Multiple $R = 0.70$; $R^2 = 0.50$; Adjusted $R^2 = 0.49$					Multiple $R = 0.84$; $R^2 = 0.71$; Adjusted $R^2 = 0.65$					Multiple $R = 0.94$; $R^2 = 0.89$; Adjusted $R^2 = 0.82$				
F-statistic: $F\,(2,34) = 16.7$; F significance = < 0.05					F-statistic: $F\,(4,20) = 12.1$; F significance = < 0.05					F-statistic: $F\,(4,7) = 13.9$; F significance = < 0.05				

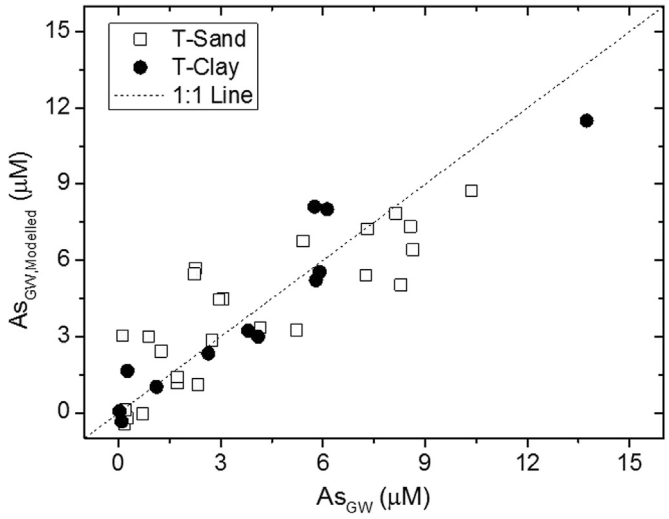

Figure 11. MLR-modelled groundwater arsenic ($As_{GW,\ Modelled}$) versus measured groundwater arsenic (As_{GW}) using refined models for T-Sand (*f*(pH, $Fe_{Sed,W}$, $As_{Sed,S}$ and TOC)) and T-Clay (*f*(pH, $Fe_{Sed,W}$, $As_{Sed,W}$ and $As_{Sed,S}$)). The subscripts Sed,W and Sed,S refer respectively to weakly bound and strong bound sedimentary concentrations of the associated chemical component.

Fe_{GW} (Multiple $R = 0.70$; $F\,(2, 34) = 16.7$; F significance < 0.05). When the dataset is split by transect, the unrefined correlations for T-Sand are stronger than for the bulk dataset (Table 4B; Multiple $R = 0.86$; $F\,(9, 15) = 4.8$; F significance < 0.05); however for T-Clay the unrefined MLR has a high multiple R but the F-statistic is not statistically significant (Table 4C; Multiple $R = 0.96$; $F\,(9, 2) = 2.8$; F significance $= 0.30$). The refined model for T-Sand (Multiple $R = 0.84$; $F\,(4, 20) = 12.1$; F significance < 0.05) depends on the explanatory variables pH, $Fe_{Sed,W}$, $As_{Sed,S}$ and TOC; in contrast the refined model for T-Clay (Multiple $R = 0.94$; $F\,(4, 7) = 13.9$; F significance < 0.05) depends on pH, $Fe_{Sed,W}$, $As_{Sed,W}$ and $As_{Sed,S}$ as statistically significantly explanatory variables for As_{GW}. Although the explanatory variables are similar for the two transects (e.g. in both transects pH, $Fe_{Sed,W}$ and $As_{Sed,S}$ are important in controlling As_{GW}), the differences (e.g. the significance of TOC in T-Sand only and of $As_{Sed,W}$ in T-Clay only) highlight distinct differences in the sorption behaviour between the two transects.

MLR-modelled values ($As_{GW,\ Modelled}$) are in good agreement with observed As_{GW} (Fig. 11), although the modelled values show a slight overestimate at low As_{GW} and a slight underestimate at high As_{GW}. The underestimate bias at high As_{GW} could speculatively be attributed to greater possible sequestering of As_{GW} via sorption/re-absorption when As_{GW} concentrations are high. Note however that a high level of prediction is not unexpected given that the MLR-models are based directly on inputs from measured groundwater chemistry within the same dataset. Ideally, a predictive multivariate model should be based on a training data subset and validated using a separate, randomly selected testing data subset; however in this case the dataset when subdivided was too small to do this reliably. Because of this limitation, this model should not be interpreted as a validated predictive model but rather solely for indicative/illustrative purposes and which could potentially be built upon with a larger dataset.

In addition to splitting the data by transects, MLR was also conducted with "Low *Eh*" and "High *Eh*" data subsets using both unrefined and refined models (Table 5). In highly reducing, low *Eh* groundwaters, As_{GW} can be described by a refined MLR model taking consideration of pH and Fe_{GW} only as explanatory variables (Table 5A; Multiple $R = 0.65$; $F\,(2, 21) = 7.7$; F significance < 0.05). The dependence of As_{GW} on pH and Fe_{GW} for low *Eh* groundwaters is similar to that of the overall dataset (Table 4A) and reflects that the majority of the groundwater in this field area is highly reducing. Interestingly, the controlling variables for As_{GW} in these typical, low *Eh* groundwaters are characteristic of the groundwater itself and the corresponding sedimentary characteristics at the same depth have no significant influence over the observed As_{GW}. In contrast, in high *Eh* groundwaters (Table 5B), none of the evaluated variables (including both aqueous and sediment characteristics) were statistically sufficient to explain As_{GW}. Although the dataset is too small to conduct robust MLR analysis for groups split by both transect and *Eh*, such analysis may be useful given a larger dataset, particularly in high *Eh* groundwaters, in order to better understand the controls on As_{GW} under those more oxidising geochemical conditions. Regardless of sample size limitations, the MLR analysis supports that the speculation that groundwater may be re-

Table 5
Summary of MLR for arsenic in groundwater conducted on the dataset split by *Eh*: (A) "Low *Eh*" < -75 mV and (B) "High *Eh*" > -75 mV. The table shows both an unrefined model with all variables and a refined model with only variables for which H_0 has been rejected at the 95% confidence level. The F-statistic is reported as *F* (regression df, residual df) = value, where df = degrees of freedom. No refined model was statistically significant with these explanatory variables for the High *Eh* group.

(A) Low *Eh* (<−75 mV)					(B) High *Eh* (>−75 mV)				
Unrefined	Estimate	Std. Error	*t* value	*P*-value	Unrefined	Estimate	Std. Error	*t* value	*P*-value
(Intercept)	−85.9	32.2	−2.7	<0.05	(Intercept)	−51.9	117	−0.4	0.69
pH	12.6	4.7	2.7	<0.05	pH	7.4	16.4	0.5	0.68
Eh (mV)	−0.01	0.03	−0.4	0.70	*Eh* (mV)	−0.01	0.05	−0.2	0.85
Fe_{GW} (µM)	0.01	0.01	1.6	0.12	Fe_{GW} (µM)	0.02	0.03	0.5	0.63
$As_{Sed,W}$ (µg/g)	0.9	10.5	0.1	0.93	$As_{Sed,W}$ (µg/g)	−4.6	7.6	−0.6	0.59
$Fe_{Sed,W}$ (µg/g)	0.0005	0.003	0.2	0.88	$Fe_{Sed,W}$ (µg/g)	0.0002	0.007	0.0	0.98
$As_{Sed,S}$ (µg/g)	−0.3	1.3	−0.2	0.84	$As_{Sed,S}$ (µg/g)	1.1	1.6	0.7	0.54
$Fe_{Sed,S}$ (µg/g)	−0.1	0.1	−0.9	0.39	$Fe_{Sed,S}$ (µg/g)	0.02	0.3	0.1	0.95
TOC (%)	3.6	2.5	1.4	0.18	TOC (%)	−0.2	2.2	−0.1	0.93
MGS (µm)	0.004	0.004	1.1	0.31	MGS (µm)	0.01	0.05	0.3	0.82
Residual standard error = 3.0 (14 df)					Residual standard error = 3.1 (3 df)				
Multiple $R = 0.73$; $R^2 = 0.53$; Adjusted $R^2 = 0.23$					Multiple $R = 0.71$; $R^2 = 0.50$; Adjusted $R^2 = -0.99$				
F-statistic: $F\,(9,14) = 1.8$; F significance = 0.16					F-statistic: $F\,(9,3) = 0.3$; F significance = 0.91				
Refined	Estimate	Std. Error	*t* value	*P*-value	Refined	Estimate	Std. Error	*t* value	*P*-value
(Intercept)	−95.7	25.6	−3.7	<0.05	*Refined model not applicable; explanatory variables are statistically insignificant*				
pH	14.0	3.6	3.9	<0.05					
Fe_{GW} (µM)	0.01	0.01	2.2	<0.05					
Residual standard error = 2.70 (21df)									
Multiple $R = 0.65$; $R^2 = 0.42$; Adjusted $R^2 = 0.37$									
F-statistic: $F\,(2,21) = 7.7$; F significance = < 0.05									

equilibrating with host sediments through sorption/desorption reactions, the extent of which may vary according to dominant aqueous and sedimentary geochemical and/or hydrological conditions. This heterogeneity is also reflected in the site-specific and seasonal variability in inorganic aqueous geochemistry and redox conditions (Richards et al., 2017a) and dominant groundwater recharge processes (Richards et al., 2018).

4. Conclusions

In a well-studied and heavily As-affected aquifer in Kandal Province, Cambodia, the concentrations of weakly and strongly bound As, Fe, Mn and P in the aquifer host sediment were compared to sediment mean grain size and associated groundwater composition in order to determine if, and to what extent, groundwater may be (partially) re-equilibrating with host sediments through sorption/desorption reactions. In general, pH and *Eh* are the dominant controls on As_{GW}, which typically increases with depth and is positively associated with Fe_{GW}. Two distinct transects, T-Sand and T-Clay, show contrasting sorption behaviour which could be attributed to differing lithology (while noting the broad distribution of grain sizes that can be present even in a sand-dominated or clay-dominated sample or transect), biogeochemical and/or hydrogeological conditions. Sorption/desorption processes appear to be re-setting groundwater As concentrations, to varying extents, in both transects but particularly in T-Clay, where the very high concentrations of weakly or strongly bound As are not necessarily directly reflected in groundwater As concentrations, where generally smaller grain size (and hence greater surface area) sedimentary sequences are located and where groundwater flows are expected to be generally slower. In T-Sand, the following observations are made: (i) As_{GW} and $Fe_{Sed,W}$ are negatively correlated, suggesting that dissolved As_{GW} may be sequestered by sorption/re-absorption onto solid phase Fe minerals; (ii) $As_{Sed,W}$ is positively correlated with both $Fe_{Sed,W}$ and sedimentary TOC, which is suggestive of the importance of sorption of As(III) to Fe-bearing mineral phases and/or TOC; and (iii) $As_{Sed,W}$ is negatively correlated with MGS which is expected given the greater specific surface areas of fine-grained sediments. In contrast, in T-Clay, the following observations hold: (i) no significant correlation between As_{GW} and $Fe_{Sed,W}$, nor between $As_{Sed,W}$ and $Fe_{Sed,W}$ (suggests different dominant processes than T-Sand); (ii) no relationship between $As_{Sed,W}$ and MGS, however a strong negative correlation between *Eh* and MGS show that the redox conditions may not be sufficiently reducing to support As mobilization in the finest grained sediments; and (iii) the wide range of observed $As_{Sed,W}$ at very low TOC may suggest a degree of binding/occlusion of As-bearing Fe-bearing minerals to the sedimentary OM. These differences are further reflected in the MLR modelling, which shows that As_{GW} in T-Sand is correlated with explanatory variables pH, $Fe_{Sed,W}$, $As_{Sed,S}$ and TOC; whereas As_{GW} in T-Clay depends on pH, $Fe_{Sed,W}$, $As_{Sed,W}$ and $As_{Sed,S}$. The important implication here is that sampled groundwater chemistry may not be representative of, and indeed may "mask", the key biogeochemical processes ultimately controlling initial As mobilization in such aquifers.

Acknowledgements

This research was funded by a NERC (Natural Environment Research Council, UK) Standard Research Grant (NE/J023833/1) to DAP, BEvD and C.J. Ballentine (now at University of Oxford) and a NERC PhD studentship (NE/L501591/1) to DM. MJCM acknowledges receipt of a University of Cádiz(UCA) Postdoctoral Bridge Contract award, and LAR acknowledges the support of The Leverhulme Trust (UK) (ECF2015-657). Louise Norman (formerly University of Manchester, UoM) is thanked for contributions to sediment extractions and Safia Bibi (formerly UoM) and Debbie Ashworth (UoM) are thanked for preparation of samples for TOC analysis. Paul Lythgoe and Karen Theis (both UoM) are thanked for analytical and laboratory support. The following people are thanked for their contributions to the field campaigns during which these samples for this study were collected: Chivuth Kong, Pheary Meas, Teyden Sok and Yut Yann (Royal University of Agriculture, Cambodia); Chhengngunn Aing and Zongta Sang (Royal University of Phnom Penh, Cambodia), local landowners and the local drilling team led by Hok Meas. Resources Development International – Cambodia is thanked for logistical support during field campaigns.

References

Al Lawati, W.M., Jean, J.-S., Kulp, T.R., Lee, M.-K., Polya, D.A., Liu, C.-C., van Dongen, B.E., 2013. Characterisation of organic matter associated with groundwater arsenic in reducing aquifers of southwestern Taiwan. Journal of Hazardous Materials 262, 970–979.

Al Lawati, W.M., Rizoulis, A., Eiche, E., Boothman, C., Polya, D.A., Lloyd, J.R., Berg, M., Vasquez-Aguilar, P., van Dongen, B.E., 2012a. Characterisation of organic matter and microbial communities in contrasting arsenic-rich Holocene and arsenic-poor Pleistocene aquifers, Red River Delta, Vietnam. Applied Geochemistry 27, 315–325.

Al Lawati, W.M., van Dongen, B.E., Polya, D.A., Jean, J.S., Kulp, T.R., Berg, M., 2012b. The effects of organics on the transformation and release of arsenic. In: NG, J.C., Noller, B.N., Naidu, R., Bundschuh, J., Bhattacharya, P. (Eds.), Understanding the Geological and Medical Interface of Arsenic. Arsenic 2012.

Anawar, H.M., Mihaljevič, M., Garcia-Sanchez, A., Akai, J., Moyano, A., 2010. Investigation of sequential chemical extraction of arsenic from sediments: variations in sample treatment and extractant. Soil and Sediment Contamination: International Journal 19, 133–141.

Benner, S.G., Polizzotto, M.L., Kocar, B.D., Ganguly, S., Phan, K., Ouch, K., Sampson, M., Fendorf, S., 2008. Groundwater flow in an arsenic-contaminated aquifer, Mekong Delta, Cambodia. Applied Geochemistry 23, 3072–3087.

Blott, S.J., Pye, K., 2001. GRADISTAT: a grain size distribution and statistics package for the analysis of unconsolidated sediments. Earth Surface Processes and Landforms 26, 1237–1248.

Brodie, C.R., Leng, M.J., Casford, J.S.L., Kendrick, C.P., Lloyd, J.M., Yongqiang, Z., Bird, M.I., 2011. Evidence for bias in C and N concentrations and $\delta^{13}C$ composition of terrestrial and aquatic organic materials due to pre-analysis acid preparation methods. Chemical Geology 282, 67–83.

Casanueva-Marenco, M.J., Magnone, D., Richards, L.A., Polya, D.A., 2016. Selective chemical extractions of Cambodian aquifer sediments - evidence for sorption processes controlling groundwater arsenic. In: Arsenic Research and Global Sustainability: Proceedings of the 6th International Congress on Arsenic in the Environment. Stockholm, Sweden, pp. 76–77.

Charlet, L., Polya, D.A., 2006. Arsenic in shallow, reducing groundwaters in southern Asia: an environmental health disaster. Elements 2, 91–96.

Diwakar, J., Johnston, S.G., Burton, E.D., Das Shrestha, S., 2015. Arsenic mobilization in an alluvial aquifer of the Terai region, Nepal. Journal of Hydrology: Regional Studies 4, 59–79.

Dixit, S., Hering, J.G., 2003. Comparison of arsenic(V) and arsenic(III) sorption onto iron oxide minerals: implications for arsenic mobility. Environmental Science and Technology 37, 4182–4189.

Duan, L., Song, J., Yuan, H., Li, X., Li, N., 2013. Spatio-temporal distribution and environmental risk of arsenic in sediments of the East China Sea. Chemical Geology 340, 21–31.

Eiche, E., Neumann, T., Berg, M., Weinman, B., van Geen, A., Norra, S., Berner, Z., Trang, P.T.K., Viet, P.H., Stüben, D., 2008. Geochemical processes underlying a sharp contrast in groundwater arsenic concentrations in a village on the Red River delta, Vietnam. Applied Geochemistry 23, 3143–3154.

Feng, Q., Zhang, Z., Chen, Y., Liu, L., Zhang, Z., Chen, C., 2013. Adsorption and desorption characteristics of arsenic on soils: kinetics, equilibrium, and effect of $Fe(OH)_3$ colloid, H_2SiO_3 colloid and phosphate. Procedia Environmental Sciences 18, 26–36.

Goldberg, S., Criscenti, L.J., Turner, D.R., Davis, J.A., Cantrell, K.J., 2007. Adsorption-desorption processes in subsurface reactive transport modelling. Vadose Zone Journal 6, 407–435.

Islam, F.S., Gault, A.G., Boothman, C., Polya, D.A., Charnock, J.M., Chatterjee, D., Lloyd, J.R., 2004. Role of metal-reducing bacteria in arsenic release from Bengal delta sediments. Nature 430, 68–71.

Javed, M.B., Kachanoski, G., Siddique, T., 2013. A modified sequential extraction method for arsenic fractionation in sediments. Analytica Chimica Acta 787, 102–110.

Johnson, K., Purvis, G., Lopez-Capel, E., Peacock, C., Gray, N., Wagner, T., März, C., Bowen, L., Ojeda, J., Finlay, N., Robertson, S., Worrall, F., Greenwell, C., 2015. Towards a mechanistic understanding of carbon stabilization in manganese oxides. Nature Communications 6.

Kaiser, K., Guggenberger, G., 2000. The role of DOM sorption to mineral surfaces in the preservation of organic matter in soils. Organic Geochemistry 31, 711–725.
Keon, N.E., Swartz, C.H., Brabander, D.J., Harvey, C., Hemond, H.F., 2001. Validation of an arsenic sequential extraction method for evaluating mobility in sediments. Environmental Science and Technology 35, 2778–2784.
Kim, E.J., Lee, J.-C., Baek, K., 2015. Abiotic reductive extraction of arsenic from contaminated soils enhanced by complexation: arsenic extraction by reducing agents and combination of reducing and chelating agents. Journal of Hazardous Materials 283, 454–461.
Kim, S.-H., Kim, K., Ko, K.-S., Kim, Y., Lee, K.-S., 2012. Co-contamination of arsenic and fluoride in the groundwater of unconsolidated aquifers under reducing environments. Chemosphere 87, 851–856.
Kocar, B.D., Polizzotto, M.L., Benner, S.G., Ying, S.C., Ung, M., Ouch, K., Samreth, S., Suy, B., Phan, K., Sampson, M., Fendorf, S., 2008. Integrated biogeochemical and hydrologic processes driving arsenic release from shallow sediments to groundwaters of the Mekong delta. Applied Geochemistry 23, 3059–3071.
Lalonde, K., Mucci, A., Ouellet, A., Gélinas, Y., 2012. Preservation of organic matter in sediments promoted by iron. Nature 483, 198–200.
Lawson, M., Polya, D.A., Boyce, A.J., Bryant, C., Ballentine, C.J., 2016. Tracing organic matter composition and distribution and its role on arsenic release in shallow Cambodian groundwaters. Geochimica et Cosmochimica Acta 178, 160–177.
Lawson, M., Polya, D.A., Boyce, A.J., Bryant, C., Mondal, D., Shantz, A., Ballentine, C.J., 2013. Pond-derived organic carbon driving changes in arsenic hazard found in Asian groundwaters. Environmental Science and Technology 47, 7085–7094.
Li, H., Shi, A., Zhang, X., 2015. Particle size distribution and characteristics of heavy metals in road-deposited sediments from Beijing Olympic Park. Journal of Environmental Sciences 32, 228–237.
Magnone, D., Richards, L.A., Polya, D.A., Bryant, C., Jones, M., van Dongen, B.E., 2017. Biomarker-indicated extent of oxidation of plant-derived organic carbon (OC) in relation to geomorphology in an arsenic contaminated Holocene aquifer, Cambodia. Scientific Reports 7. https://doi.org/10.1038/s41598-017-13354-8.
Mai, N.T.H., Postma, D., Trang, P.T.K., Jessen, S., Viet, P.H., Larsen, F., 2014. Adsorption and desorption of arsenic to aquifer sediment on the red river floodplain at nam du, vietnam. Geochimica et Cosmochimica Acta 142, 587–600.
Mayorga, P., Moyano, A., Anawar, H.M., García-Sánchez, A., 2013. Temporal variation of arsenic and nitrate content in groundwater of the Duero River Basin (Spain). Physics and Chemistry of the Earth 58 – 60, 22–27.
Meng, X., Dupont, R.R., Sorensen, D.L., Jacobson, A.R., Mclean, J.E., 2017. Mineralogy and geochemistry affecting arsenic solubility in sediment profiles from the shallow basin-fill aquifer of Cache Valley Basin, Utah. Applied Geochemistry 77, 126–141.
Michael, H.A., Voss, C.I., 2008. Evaluation of the sustainability of deep groundwater as an arsenic-safe resource in the Bengal Basin. Proceedings of the National Academy of Sciences 105, 8531–8536.
Miller, J.N., Miller, J.C., 2010. Chapter 5: Calibration Methods in Instrumental Analysis: Regression and Correlation. Statistics and Chemometrics for Analytical Chemistry. Pearson Education.
Papacostas, N.C., Bostick, B., Quicksall, A.N., Landis, J.D., Sampson, M., 2008. Geomorphic controls on groundwater arsenic distribution in the Mekong River Delta, Cambodia. Geology 36, 891–894.
Paul, D., Kazy, S.K., Banerjee, T.D., Gupta, A.K., Pal, T., Sar, P., 2015. Arsenic biotransformation and release by bacteria indigenous to arsenic contaminated groundwater. Bioresource Technology 188, 14–23.
Peters, S.C., 2008. Arsenic in groundwaters in the Northern Appalachian Mountain belt: a review of patterns and processes. Journal of Contaminant Hydrology 99, 8–21.
Phan, K., Phan, S., Heng, S., Huoy, L., Kim, K.-W., 2014. Assessing arsenic intake from groundwater and rice by residents in Prey Veng province, Cambodia. Environmental Pollution 185, 84–89.
Polizzotto, M.L., Kocar, B.D., Benner, S.G., Sampson, M., Fendorf, S., 2008. Near-surface wetland sediments as a source of arsenic release to ground water in Asia. Nature 454, 505–508.
Polya, D.A., Charlet, L., 2009. Rising arsenic risk? Nature Geoscience 2, 383–384.
Polya, D.A., Gault, A.G., Bourne, N.J., Lythgoe, P.R., Cooke, D.A., 2003. Coupled HPLC-ICP-MS Analysis Indicates Highly Hazardous Concentrations of Dissolved Arsenic Species in Cambodian Groundwaters, vol. 288. Royal Society of Chemistry Special Publication, pp. 127–140.
Polya, D.A., Gault, A.G., Diebe, N., Feldman, P., Rosenboom, J.W., Gilligan, E., Fredericks, D., Milton, A.H., Sampson, M., Rowland, H.A.L., Lythgoe, P.R., Jones, J.C., Middleton, C., Cooke, D.A., 2005. Arsenic hazard in shallow Cambodian groundwaters. Mineralogical Magazine 69, 807–823.
Polya, D.A., Lawson, M., 2015. Chapter 2: geogenic and anthropogenic arsenic hazard in groundwaters and soils. In: States, C. (Ed.), Arsenic: Exposure Sources, Health Risks and Mechanisms of Toxicity. Wiley.
Polya, D.A., Middleton, D.R.S., 2017. Chapter 1: arsenic in drinking water: sources & human exposure. In: Bhattacharya, P., Polya, D.A., Jovanovic, D. (Eds.), Best Practice Guide on the Control of Arsenic in Drinking Water. IWA Publishing, ISBN 9781843393856.
Polya, D.A., Mondal, D., Ganguli, B., Giri, A.K., Banerjee, M., Khattak, S., Phawadee, N., Sovann, C., 2010. Geogenic arsenic in groundwaters and soils – re-evaluating exposure routes and risk assessment. In: Bhattacharya, P., Rosborg, I., Sandhi, A., Hayes, C., Benoliel, M.J. (Eds.), Metals and Related Substances in Drinking Water, vol. 536. COST Action.
Polya, D.A., Richards, L.A., Al Bualy, A.N., Sovann, C., Magnone, D., Lythgoe, P.R., 2017. Chapter A14: groundwater sampling, arsenic analysis and risk communication: Cambodia Case Study. In: Bhattacharya, P., Polya, D.A., Jovanovic, D. (Eds.), Best Practice Guide for the Control of Arsenic in Drinking Water. IWA Publishing, ISBN 9781843393856.
Polya, D.A., Watts, M.J., 2017. Chapter 5: sampling and analysis for monitoring arsenic in drinking water. In: Bhattacharya, P., Polya, D.A., Jovanovic, D. (Eds.), Best Practice Guide on the Control of Arsenic in Drinking Water. IWA Publishing, ISBN 9781843393856.
Radloff, K.A., Zheng, Y., Michael, H.A., Stute, M., Bostick, B.C., Mihajlov, I., Bounds, M., Huq, M.R., Choudhury, I., Rahman, M.W., Schlosser, P., Ahmed, K.M., van Geen, A., 2011. Arsenic migration to deep groundwater in Bangladesh influenced by adsorption and water demand. Nature Geoscience 4, 793–798.
Ravenscroft, P., Brammer, H., Richards, K., 2009. Arsenic Pollution - A Global Synthesis. Wiley-Blackwell, Chichester.
Richards, L.A., Magnone, D., Boyce, A.J., Casanueva-Marenco, M.J., van Dongen, B.E., Ballentine, C.J., Polya, D.A., 2018. Delineating sources of groundwater recharge in an arsenic-affected holocene aquifer in Cambodia using stable isotope-based mixing models. Journal of Hydrology 557, 321–324.
Richards, L.A., Magnone, D., Sovann, C., Kong, C., Uhlemann, S., Kuras, O., van Dongen, B.E., Ballentine, C.J., Polya, D.A., 2017a. High resolution profile of inorganic aqueous geochemistry and key redox zones in an arsenic bearing aquifer in Cambodia. The Science of the Total Environment 590–591, 540–553.
Richards, L.A., Magnone, D., van Dongen, B.E., Ballentine, C.J., Polya, D.A., 2015. Use of lithium tracers to quantify drilling fluid contamination for groundwater monitoring in Southeast Asia. Applied Geochemistry 63, 190–202.
Richards, L.A., Sültenfuß, J., Ballentine, C.J., Magnone, D., van Dongen, B.E., Sovann, C., Polya, D.A., 2017b. Tritium tracers of rapid surface water ingression into arsenic-bearing aquifers in the lower Mekong basin, Cambodia. Procedia Earth and Planetary Science 17C, 849–852.
Rowland, H.A.L., Gault, A.G., Lythgoe, P., Polya, D.A., 2008. Geochemistry of aquifer sediments and arsenic-rich groundwaters from Kandal Province, Cambodia. Applied Geochemistry 23, 3029–3046.
Roy, M., Mcmanus, J., Goñi, M.A., Chase, Z., Borgeld, J.C., Wheatcroft, R.A., Muratli, J.M., Megowan, M.R., Mix, A., 2013. Reactive iron and manganese distributions in seabed sediments near small mountainous rivers off Oregon and California (USA). Continental Shelf Research 54, 67–79.
Smedley, P.L., Kinniburgh, D.G., 2002. A review of the source, behaviour and distribution of arsenic in natural waters. Applied Geochemistry 17, 517–568.
Smith, A.H., Lingas, E.O., Rahman, M., 2000. Contamination of drinking-water by arsenic in Bangladesh: a public health emergency. Bulletin of the World Health Organization 78, 1093–1103.
Stuckey, J.W., Schaefer, M.V., Benner, S.G., Fendorf, S., 2015a. Reactivity and speciation of mineral-associated arsenic in seasonal and permanent wetlands of the Mekong Delta. Geochimica et Cosmochimica Acta 171, 143–155.
Stuckey, J.W., Schaefer, M.V., Kocar, B.D., Benner, S.G., Fendorf, S., 2016. Arsenic release metabolically limited to permanently water-saturated soil in Mekong Delta. Nature Geoscience 9, 70–76.
Stuckey, J.W., Schaefer, M.V., Kocar, B.D., Dittmar, J., Pacheco, J.L., Benner, S.G., Fendorf, S., 2015b. Peat formation concentrates arsenic within sediment deposits of the Mekong Delta. Geochimica et Cosmochimica Acta 149, 190–205.
Tamura, T., Saito, Y., Sieng, S., Ben, B., Kong, M., Choup, S., Tsukawaki, S., 2007. Depositional facies and radiocarbon ages of a drill core from the Mekong River lowland near Phnom Penh, Cambodia: evidence for tidal sedimentation at the time of Holocene maximum flooding. Journal of Asian Earth Sciences 29, 585–592.
Uhlemann, S., Kuras, O., Richards, L.A., Naden, E., Polya, D.A., 2017. Electrical Resistivity Tomography determines the spatial distribution of clay layer thickness and aquifer vulnerability, Kandal Province, Cambodia. Journal of Asian Earth Sciences 147, 402–414.
Ure, A.M., Quevauviller, P., Muntau, H., Griepink, B., 1993. Speciation of heavy metals in soils and sediments. An account of the improvement and harmonization of extraction techniques undertaken under the auspices of the BCR of the commission of the european communities. International Journal of Environmental Analytical Chemistry 51, 135–151.
van Dongen, B., Rowland, H.A.L., Gault, A.G., Polya, D.A., Bryant, C., Pancost, R.D., 2008. Hopane, sterane and n-alkane distributions in shallow sediments hosting high arsenic groundwaters in Cambodia. Applied Geochemistry 23, 3047–3058.
van Geen, A., Bostick, B.C., Trang, P.T.K., Lan, V.M., Mai, N.-N., Manh, P.D., Viet, P.H., Radloff, K.A., Aziz, Z., Mey, J.L., Stahl, M.O., Harvey, C.F., Oates, P., Weinman, B., Stengel, C., Frei, F., Kipfer, R., Berg, M., 2013. Retardation of arsenic transport through a Pleistocene aquifer. Nature 501, 204–207.
Vandenbroucke, M., Largeau, C., 2007. Review: kerogen origin, evolution and structure. Organic Geochemistry 38, 719–833.
Wang, Y., Xie, X., Johnson, T.M., Lundstrom, C.C., Ellis, A., Wang, X., Duan, M., Li, J., 2014. Coupled iron, sulfur and carbon isotope evidences for arsenic enrichment in groundwater. Journal of Hydrology 519, 414–422.
World Health Organization, 2011. Guidelines for Drinking-Water Quality, fourth ed. Geneva.
Xie, X., Ellis, A., Wang, Y., Xie, Z., Duan, M., Su, C., 2009. Geochemistry of redox-sensitive elements and sulfur isotopes in the high arsenic groundwater system of Datong Basin, China. The Science of the Total Environment 407, 3823–3835.
Yadav, I.C., Devi, N.L., Singh, S., 2015. Reductive dissolution of iron-oxyhydroxides directs groundwater arsenic mobilization in the upstream of Ganges River basin, Nepal. Journal of Geochemical Exploration 148, 150–160.
Yang, Q., Culbertson, C.W., Nielsen, M.G., Schalk, C.W., Johnson, C.D., Marvinney, R.G., Stute, M., Zheng, Y., 2015. Flow and sorption controls of groundwater arsenic in individual boreholes from bedrock aquifers in central Maine, USA. The Science of the Total Environment 505, 1291–1307.